Structural stability and magnetic properties of metastable Fe-Cu alloys studied by *ab initio* calculations and molecular dynamics simulations

H. R. Gong, L. T. Kong, and B. X. Liu*

Advanced Materials Laboratory, Department of Materials Science and Engineering, Tsinghua University, Beijing 100084, China

(Received 20 May 2003; revised manuscript received 19 August 2003; published 17 February 2004)

For the equilibrium immiscible Fe-Cu system, *ab initio* calculations using the projector augmented wave method identify the relatively stable structures of the metastable $Fe_{25}Cu_{75}$ and $Fe_{50}Cu_{50}$ alloys to be both of fcc and determine their corresponding lattice constants and cohesive energies. Some of the *ab initio* calculated properties are used in deriving an embedded-atom Fe-Cu potential. Based on the proven realistic potential, the structural stability of the Fe_xCu_{100-x} alloy is studied for the entire composition range of the system through molecular dynamics simulations. The simulations predict that a fcc structure is more stable than a bcc one when $0 \leqslant x \leqslant 60$, while the bcc structure becomes energetically favored when $60 < x \leqslant 100$, and that the prediction confirms the verdict from *ab initio* calculations for the $Fe_{25}Cu_{75}$, $Fe_{50}Cu_{50}$, and $Fe_{75}Cu_{25}$ alloys. Moreover, *ab initio* calculations are also performed to determine the magnetic moments of some metastable Fe-Cu alloys and the results are reasonably compatible with the experimental observations.

DOI: 10.1103/PhysRevB.69.054203 PACS number(s): 64.60.My, 75.50.Bb, 82.20.Wt

I. INTRODUCTION

During the past decades, much attention has been drawn to the equilibrium immiscible Fe-Cu system, which is characterized by a positive heat of formation ($\Delta H_f = +19$ kJ/mol) calculated by Miedema's theory at an equiatomic stoichiometry.[1] By employing some nonequilibrium/far-from-equilibrium producing techniques, such as mechanical alloying,[2–4] ion-beam mixing,[5,6] vapor deposition,[7,8] and vapor quenching,[9] etc., a number of metastable Fe-Cu alloys have been obtained. Some of the newly obtained metastable Fe-Cu alloys feature unique magnetic properties and become potential candidate materials for practical applications.[2,7,8,10–12] As to the theoretical studies of the Fe-Cu alloys, a number of excellent research works have been published in the literature. For instance, Ma *et al.* performed thermodynamic calculations concerning the heats of formation of the fcc and bcc Fe-Cu alloys and the calculations confirmed their experimental observations from mechanical alloying.[11,13] Besides, *ab initio* calculations were used by several researchers to calculate the magnetic moments of the Fe-Cu alloys with different methods.[14–18]

It is well known that molecular dynamics (MD) simulation is a powerful means to study the metastable phase formation, as well as the phase transition of the binary metal systems at an atomic level. To the authors' knowledge, however, there is no MD simulation for the equilibrium immiscible Fe-Cu system reported in the literature. To further develop new Fe-Cu alloys with high performance, it is therefore of necessity to pursue a through theoretical investigation concerning the formation of metastable Fe-Cu alloys and the associated magnetic properties at atomic and electronic scales.

The present work is dedicated to combine the first principles (*ab initio*) calculation and molecular dynamics (MD) simulation for studying the structural stability of the possible metastable Fe-Cu alloys and the associated magnetic properties. First, *ab initio* calculations are conducted to determine the structures, lattice constants, and cohesive energies of the possible metastable Fe-Cu phases at some specific alloy compositions, i.e., $Fe_{25}Cu_{75}$ and $Fe_{50}Cu_{50}$, respectively. Second, through fitting to the *ab initio* calculated physical properties of some Fe-Cu phases, an *n*-body Fe-Cu potential is derived under the framework of an embedded-atom method (EAM). Third, applying the proven realistic Fe-Cu potential, MD simulations are performed to reveal the correlation between the structure and formation energy of the possible metastable Fe-Cu phases over the entire composition range. Fourth, *ab initio* calculations are also conducted to predict the magnetic properties of some metastable Fe-Cu alloys. We report, in this paper, the predictions concerning the structural stability and the magnetic properties of the Fe-Cu system as well as the comparison between the theoretical results and those observed in experiments.

II. THEORETICAL AND CHARACTERIZATION METHODS

A. *Ab initio* calculation

The first-principles calculations are based on the well-established Vienna *ab initio* simulation package.[19] The calculations are carried out by using the projector augmented wave (PAW) method.[20] The exchange and correlation effects are described by the functions due to Perdew and Zunger,[21] employing the generalized gradient approximation (GGA) proposed by Perdew *et al.*[22] Brillouin-zone integrations are performed using an $11 \times 11 \times 11$ Monkhorst-Pack[23] grid leading to 56 irreducible *k* points for bcc and fcc structures, respectively.

It is noted that for a unit cell in *ab initio* calculation, the variation of its atomic ratio is limited by its specific atomic configuration. In the present study, only five chemical stoichiometries, i.e., Fe_xCu_{100-x} ($x = 0$, 25, 50, 75, and 100), are therefore chosen for calculation. Meanwhile, for each chosen stoichiometry, only some simple structures are selected in the calculation, and the detailed reason for the selection has been

described in our recent publication.[24] Moreover, for the selected $Fe_{50}Cu_{50}$ phase in a fcc structure and the $Fe_{75}Cu_{25}/Fe_{25}Cu_{75}$ phase in a bcc structure, there are no such respective atomic configurations in the lists of ordered structures. We, therefore, adopt the ordered configurations proposed by Shi *et al.*[25] for the fcc $Fe_{50}Cu_{50}$ and bcc $Fe_{75}Cu_{25}/Fe_{25}Cu_{75}$ phases and their unit cells are both set to contain four atoms.

Ab initio calculations in the present work are used to study three issues. First, they are used to predict the structures, lattice constants, and cohesive energies of the ferromagnetic (FM) $Fe_{25}Cu_{75}$ and $Fe_{50}Cu_{50}$ alloys. Second, they are used to provide some physical properties of FM $Fe_{25}Cu_{75}$ and $Fe_{50}Cu_{50}$ alloys for constructing an *n*-body FM Fe-Cu potential. Meanwhile, they are also used to provide some physical properties of paramagnetic (PM) $Fe_{25}Cu_{75}$ and $Fe_{50}Cu_{50}$ alloys for constructing an *n*-body PM Fe-Cu potential. The results obtained from the two different potentials will be compared and discussed. Third, they are used to calculate the magnetic moments of some metastable Fe-Cu alloys with several simple crystalline structures.

B. Molecular dynamics simulation

Molecular dynamics (MD) simulations are carried out with Parrinello–Rahman constant pressure scheme and the equations of motion are solved through a fourth-order predictor-corrector algorithm of Gear with a time step of $t = 5 \times 10^{-15}$ s.[26] In the present study, two kinds of simulation models are employed for all the Fe-Cu phases, i.e., a fcc solid solution model consisting of $7 \times 7 \times 7 \times 4 = 1372$ atoms, and a bcc solid solution model containing $8 \times 8 \times 8 \times 2 = 1024$ atoms. In all the simulation models, the [100], [010], and [001] atomic crystal directions are parallel to the *x*, *y*, and *z* axes, respectively, and periodic boundary conditions are adopted in three dimensions.

In the fcc (bcc) solid solution model, to obtain a specific chemical stoichiometry for an Fe-Cu alloy phase, a desired number of Cu (Fe) atoms are randomly substituted by Fe (Cu) atoms in the model. It should be noted that the substituted atoms are randomly located in the positions by the random numbers, which are generated by a computer program. The different random numbers may result in somewhat different initial atomic configurations, which may have some effects on the MD simulation results (in the present study, such effects are tested to be very limited). We, therefore, perform several (3–5) different initial random structures for a specific stoichiometry, and the final physical properties of the MD simulation are from the average of the simulation results obtained from different initial random structures.

The present MD simulations are conducted to study the structural stability of the metastable Fe-Cu alloys in two aspects. One is to run the fcc/bcc solid solution models at 0 K for 20 000 MD time steps. The purpose of this simulation is to retain and relax the fcc/bcc lattices, in order to obtain the lattice constants and heats of formation of the metastable fcc/bcc Fe-Cu alloys over an entire composition range. Thus, the simulation results can show that whether a fcc or a bcc structure is energetically favored at a specific composition.

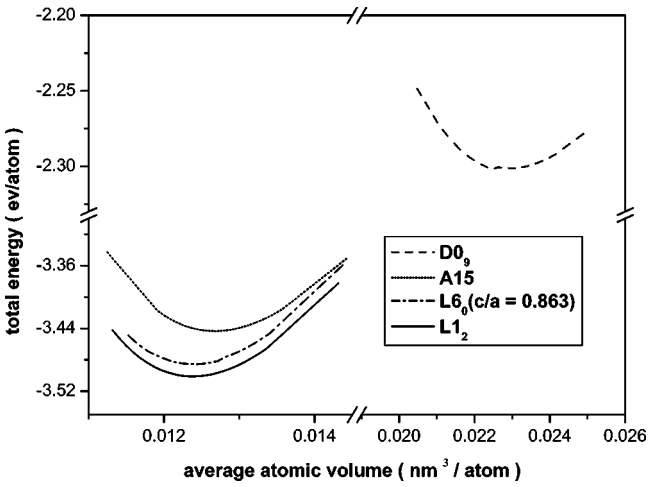

FIG. 1. The *ab initio* calculated total energy vs average atomic volume for the FM $Fe_{25}Cu_{75}$ metastable phase with different structures.

The other aspect is to run the fcc/bcc solid solution models at 300 K for adequate MD time steps until all the dynamic parameters do not show any secular variation. The purpose of this simulation is to find out whether or not the fcc/bcc Fe-Cu alloy at a specific composition can retain its structure, and to find out whether or not it can turn into an amorphous state.

III. RESULTS AND DISCUSSION

A. Prediction of metastable Fe-Cu phases

Ab initio calculations are performed to predict the structures, lattice constants, and cohesive energies of two metastable FM Fe-Cu phases, with alloy compositions of $Fe_{25}Cu_{75}$ and $Fe_{50}Cu_{50}$. As mentioned above, only simple structures are selected in the calculations and they are the A15, $D0_9$, $L1_2$, and $L6_0$ structures for the $Fe_{25}Cu_{75}$ phase, and the B1, B2, B3, and fcc structures for the $Fe_{50}Cu_{50}$ phase, respectively. Accordingly, the correlations between the total energy and average atomic volume for the $Fe_{25}Cu_{75}$ and $Fe_{50}Cu_{50}$ phases with different simple structures are obtained and displayed in Figs. 1 and 2, respectively. One sees clearly from the figures that the metastable $Fe_{25}Cu_{75}$ phase with an $L1_2$ structure (fcc type) and the metastable $Fe_{50}Cu_{50}$ phase with a fcc structure have the respectively lowest total energies among the calculated structures and are therefore predicted to be likely formed under some appropriate conditions. Accordingly, *ab initio* calculations show that the lattice constants of the $L1_2$ $Fe_{25}Cu_{75}$ and the fcc $Fe_{50}Cu_{50}$ phases are 3.65 and 3.63 Å, respectively, and their cohesive energies are 3.50 and 3.75 eV/atom, respectively.

It is of interest to note that there have been some experimental observations, which are in support of the above predictions.[2–4,7,10,11] In fact, a fcc $Fe_{25}Cu_{75}$ alloy and a fcc $Fe_{50}Cu_{50}$ alloy were indeed obtained by mechanical alloying[2–4,11] and vapor deposition,[7,10] which are both nonequilibrium producing techniques and capable of providing some energy for forming the highly energetic metastable al-

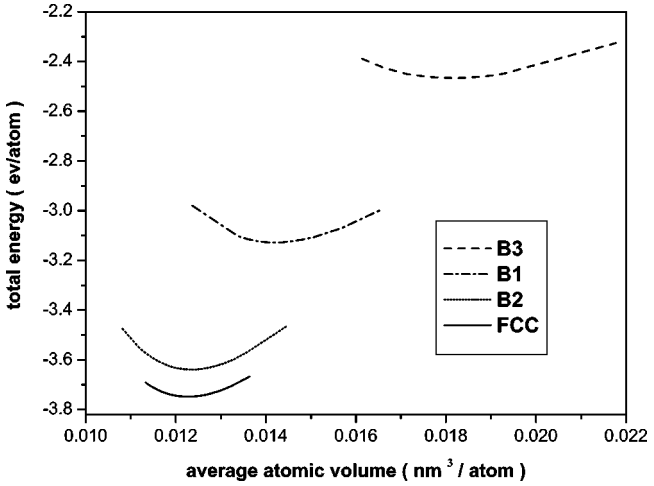

FIG. 2. The *ab initio* calculated total energy vs average atomic volume for the FM $Fe_{50}Cu_{50}$ metastable phase with different structures.

loys. Moreover, the lattice constants of the fcc $Fe_{25}Cu_{75}$ alloy and the fcc $Fe_{50}Cu_{50}$ alloy determined by diffraction analysis in experiments were 3.63 and 3.64 Å,[11] respectively, which are in excellent agreement with the values of 3.65 and 3.63 Å, respectively, predicted by the above *ab initio* calculations.

B. Construction of an *n*-body FM Fe-Cu potential

In the literature, two Fe-Cu potentials have been published so far. One is a Finnis–Sinclair potential constructed by Ackland *et al.* and has been used to study the point defect properties of the dilute Fe-Cu alloys.[27] The other is a pair potential derived by Osetsky *et al.* and has been used in simulating the copper precipitates in α-Fe.[28] It is well known that an embedded-atom method (EAM) is one of the most realistic methods to construct *n*-body potentials and is capable of reproducing some important physical properties of the transition metals and alloys with improved precision.[29–31] In the present study, we, therefore, construct an EAM Fe-Cu potential, considering the ferromagnetic property of Fe, to investigate the structural stability of the metastable Fe-Cu alloys and we will compare the newly constructed EAM potential with those reported earlier.[27,28]

The Fe-Fe and Cu-Cu potentials take the function forms adopted by Johnson and Cai,[30,31] respectively, yet with some modifications proposed by the authors. For improving the precision, the density function form of the Fe-Fe potential is set, in the present study, to be the same as that of the Cu-Cu potential. The cutoff function takes the polynomial proposed by Guellil[32] and the cutoff distances are between the second- and third-neighbor distances. In the present function forms of the potentials,[30,31] there are totally five parameters (χ,k_0,k_1,k_2,k_3) to be fitted for the Fe-Fe potential and also five parameters $(\chi,\alpha,\beta,r_a,F_1)$ to be fitted for the Cu-Cu potential. The Fe-Cu cross potential takes a combination of the Fe-Fe and Cu-Cu potentials and has the same function form proposed recently by the present authors in constructing the *n*-body Cu-Ta potential:[33]

$$\phi_{\mathrm{FeCu}}(r)=A[\phi_{\mathrm{Fe}}(r+B)+\phi_{\mathrm{Cu}}(r+C)], \tag{1}$$

where r is the distance between the Fe and Cu atoms. A, B, and C are three potential parameters to be fitted. It should be pointed out that the fitting of the Fe-Cu cross potential is a challenging issue, as in the equilibrium immiscible Fe-Cu system, there is no any equilibrium alloy phase and therefore no indispensable data available for fitting the cross potential. We, therefore, use the *ab initio* calculated cohesive energies and lattice constants of the metastable FM $L1_2$ $Fe_{25}Cu_{75}$ and B2 $Fe_{50}Cu_{50}$ phases to fit the Fe-Cu cross potential. After the fitting procedure and optimization, Table I lists the fitted potential parameters and Table II lists the comparison of the results obtained from the constructed FM Fe-Cu potentials and from experiments/*ab initio* calculations, respectively. It can be seen clearly from Table II that the present EAM Fe-Fe and Cu-Cu potentials could reproduce almost the exact values of some physical properties of pure Fe and Cu, such as cohesive energies, lattice constants, bulk modulus, elastic constants and vacancy formation energies, and that they give better results than the Finnis–Sinclair potential reported earlier.[27] Moreover, it can be noticed from Table II that the Fe-Cu cross potential is also relevant for a satisfactory description of the metastable $Fe_{25}Cu_{75}$ and $Fe_{50}Cu_{50}$ alloys.

We now turn to further testify to the relevance of the constructed FM Fe-Cu potential by performing MD simulation and *ab initio* calculation to obtain some physical properties of another metastable $Fe_{75}Cu_{25}$ phase with a bcc structure, whose physical properties have not been used in fitting the Fe-Cu potential. In the MD simulation, the bcc solid solution model is employed and subjected to annealing at 300 K for an adequate time. The simulation results predict

TABLE I. Fitted parameters for the FM Fe-Fe, Cu-Cu, and Fe-Cu potentials.

Fe-Fe		Cu-Cu		Fe-Cu	
χ	4.509 144	χ	11.134 231	A	0.453 151
k_0 (eV)	−0.271 183	α (eV)	0.725 977		
k_1 (eV)	−0.931 581	β	3.457 434	B (Å)	0.089 827
k_2 (eV)	9.615 043	r_a (Å)	1.629 356		
k_3 (eV)	−13.477 284	F_1 (eV)	0.676 073	C (Å)	−0.121 550
r_s (Å)	2.9	r_s (Å)	3.7		
r_c (Å)	3.8	r_c (Å)	4.4		
n	0.440 653	n	0.333 333		

TABLE II. Comparison between fitted values from the FM Fe-Cu potential and experimental data/*ab initio* calculation results of the cohesive energy E_c (eV/atom), lattice constant a (Å), bulk modulus B (Mbar), elastic constants (Mbar), and vacancy formation energy E_v^f (eV) in the Fe-Cu system.

Phase	Structure	Method	E_c (eV/atom)	a (Å)	B (Mbar)	C_{11} (Mbar)	C_{12} (Mbar)	C_{44} (Mbar)	E_v^f (eV)
Fe	bcc	Expt.[a,b]	4.29	2.866 45	1.73	2.431	1.381	1.219	1.79
		Other work[c]	4.316	2.8665	1.78	2.43	1.45	1.16	1.89
		This work	4.29	2.866 48	1.73	2.431	1.381	1.219	1.79
Cu	fcc	Expt.[d]	3.54	3.615	1.38	1.70	1.225	0.758	1.30
		Other work[c]	3.519	3.615	1.37	1.68	1.21	0.75	
		This work	3.54	3.615	1.38	1.70	1.225	0.758	1.30
$Fe_{25}Cu_{75}$	$L1_2$	*Ab initio*	3.50	3.65	1.31				
		Fitted	3.53	3.65	1.18				
$Fe_{50}Cu_{50}$	B2	*Ab initio*	3.64	2.89	1.39				
		Fitted	3.59	2.89	1.48				

[a]Reference 30.
[b]Reference 34.
[c]Reference 27.
[d]Reference 31.

that the $Fe_{75}Cu_{25}$ solid solution could retain its bcc structure, which is in good agreement with the fact that a metastable $Fe_{75}Cu_{25}$ alloy of a bcc structure was indeed obtained in experiments by different methods.[2,4,7,11] Accordingly, some physical properties of the metastable bcc $Fe_{75}Cu_{25}$ phase obtained from MD simulation at 0 K, *ab initio* calculation, and experiments, respectively, are listed in Table III for comparison. One sees clearly from Table III that the cohesive energies derived from MD simulation and *ab initio* calculation match well with each other. Moreover, the lattice constant of the bcc $Fe_{75}Cu_{25}$ phase from MD simulation is 2.88 Å, which is also in exact agreement with the value predicted by *ab initio* calculation as well as with the experimentally determined one.[11] It is worthwhile mentioning again that the properties of the bcc $Fe_{75}Cu_{25}$ phase obtained from *ab initio* calculation have not been used in fitting the Fe-Cu cross potential. Consequently, the above agreements shown in Table III for the $Fe_{75}Cu_{25}$ phase among the *ab initio* calculation, MD simulation, and experiments can lend firm support to the relevance of the constructed FM Fe-Cu potential.

TABLE III. The structures, lattice constants a (Å), and cohesive energies E_c (eV/atom) of the $Fe_{75}Cu_{25}$, $Fe_{50}Cu_{50}$, and $Fe_{25}Cu_{75}$ phases derived from *ab initio* calculation, MD simulation (0 K) with the FM Fe-Cu potential, and experiments, respectively.

Phase	Method	Structure	a (Å)	E_c (eV/atom)
$Fe_{75}Cu_{25}$	*Ab initio*	bcc	2.88	3.95
	MD	bcc	2.88	3.95
	Expt.	bcc[a,b,c]	2.88[c]	
$Fe_{50}Cu_{50}$	*Ab initio*	fcc	3.63	3.75
	MD	fcc	3.66	3.71
	Expt.	fcc[a,b,c]	3.64[c]	
$Fe_{25}Cu_{75}$	*Ab initio*	$L1_2$	3.65	3.50
	MD	fcc	3.63	3.58
	Expt.	fcc[a,b,c]	3.63[c]	

[a]Reference 2.
[b]Reference 7.
[c]Reference 11.

C. Structural stability of metastable Fe-Cu phases

Applying the constructed FM Fe-Cu potential, MD simulations are performed to study the structural stability of the metastable Fe-Cu phases. First, the fcc and bcc Fe-Cu phases over the entire composition range are simulated at 0 K, respectively, to find out whether a fcc or a bcc structure is energetically favored at a specific composition. In comparison, a paramagnetic (PM) Fe-Cu potential is also constructed and to run MD simulation at 0 K, in order to find out whether or not the structural stability revealed by the FM Fe-Cu potential can be reproduced by the PM Fe-Cu potential. Second, we present in detail the simulation results at some specific compositions, i.e., $Fe_{50}Cu_{50}$, $Fe_{25}Cu_{75}$, $Fe_{90}Cu_{10}$, and $Fe_{30}Cu_{70}$, and compare the simulation results with those from *ab initio* calculations/experiments. Finally, we discuss a little bit and show from MD simulations that the so-called solid-state amorphization (SSA) is hardly to take place in the immiscible Fe-Cu system.

As MD simulation is capable of studying the structural stability of the alloy phases over the entire composition range of a system, the Fe_xCu_{100-x} solid solutions with fcc and bcc structures, respectively, are therefore simulated at 0 K, i.e., the formation energies and lattice constants of a fcc as well as a bcc Fe-Cu phase are calculated as a function of the alloy composition by the MD simulations with the FM Fe-Cu potential. Consequently, Fig. 3 shows the MD simu-

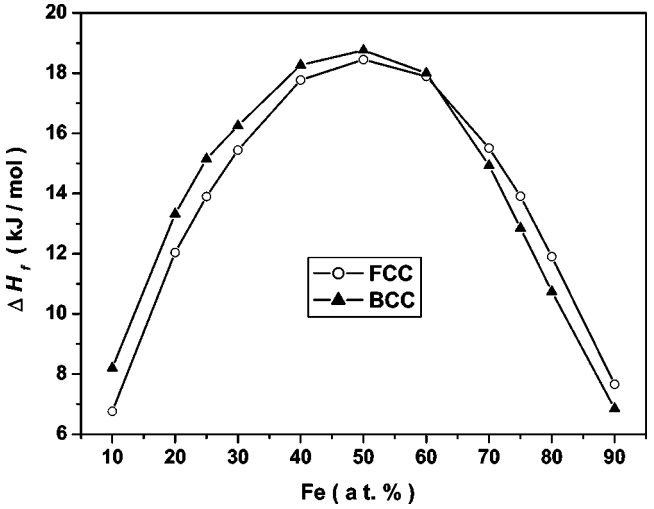

FIG. 3. The MD simulation (0 K) results of heat of formation (ΔH_f) vs the Fe concentration for the metastable FM fcc and bcc Fe-Cu phases, respectively.

lation results of the heat of formation (ΔH_f) versus the Fe concentration for the metastable FM fcc and bcc Fe-Cu phases, respectively. One sees clearly from Fig. 3 that for the case of $0 \leqslant x \leqslant 60$, the fcc Fe_xCu_{100-x} phase has lower ΔH_f and is more stable than the bcc phase, whereas for the case of $60 < x \leqslant 100$, the bcc Fe_xCu_{100-x} phase becomes energetically favored. In experiments, there have also been some observations,[2–4,7,11–13] which are in support of the above simulation results. For instance, Yavari *et al.* prepared the Fe_xCu_{100-x} alloys by mechanical alloying and found that the obtained Fe_xCu_{100-x} alloys exhibited fcc structures when $0 \leqslant x \leqslant 60$ and had bcc structures when $60 < x \leqslant 100$,[2] which are identical to the predictions by the present simulation. Eckert *et al.* found that the sputter-deposited Fe_xCu_{100-x} alloys exhibited fcc structures when $0 \leqslant x \leqslant 60$ and bcc structures when $80 \leqslant x \leqslant 100$,[3] which are also in good agreement with the present simulation results.

Thermodynamically, Ma and Aztmon[11,13] employed the CALPHAD method to obtain the enthalpy curves of the metastable FM fcc and bcc Fe-Cu solid solutions, showing that there existed a fcc-bcc transition near the Fe composition of $x = 60\%$, which are in excellent agreement with the present simulated curves shown in Fig. 3. Moreover, they also found that the fcc and bcc enthalpy curves did not intersect, if the magnetic contributions were not included in the thermodynamic functions, i.e., there was no fcc-bcc transition in the enthalpy curves of the paramagnetic fcc and bcc Fe-Cu solid solutions. It is, therefore, of interest to see whether or not this thermodynamic prediction can be reproduced in the present MD simulation. For this purpose, we also construct an *n*-body paramagnetic (PM) Fe-Cu potential under the EAM method through fitting to the lattice constants and cohesive energies of the PM $L1_2$ $Fe_{25}Cu_{75}$ and B2 $Fe_{50}Cu_{50}$ phases based on *ab initio* calculation. The construction process is similar to the description in Sec. III B and here we only list the fitted results in Table IV. Applying the constructed PM Fe-Cu potential, MD simulation is performed for the PM fcc and bcc Fe-Cu solid solutions at 0 K and the calculated heats of formation show that there is no intersection between the fcc and bcc curves, suggesting that there is no fcc-bcc transition, if the magnetic contributions of the Fe-Cu phases are not taken into account. Apparently, such MD simulation results are consistent with the thermodynamic calculations.[11,13] We now discuss a little bit about the fcc-bcc transition revealed by the FM Fe-Cu potential. As seen in Tables II and IV, the magnetic contributions lower the equilibrium energies of the Fe-Cu phases and enlarge their equilibrium lattice constants (corresponding to the magnetovolume effect[17,18]). However, as the magnetic properties of bcc and fcc Fe-Cu phases at various compositions are somewhat different,[11] the reduced energies due to the magnetic contributions are quantitatively different for the Fe-Cu phase at different stoicheometries, or with different structures (bcc or fcc). It is therefore understandable that, while including the magnetic contributions, the ΔH_f curves would change to feature an intersection suggesting a fcc-bcc transition.

We now turn to present some results of the MD simulation with the FM Fe-Cu potential at some specific compositions, i.e., $Fe_{50}Cu_{50}$, $Fe_{25}Cu_{75}$, $Fe_{90}Cu_{10}$, and $Fe_{30}Cu_{70}$. As described in Sec. III A, *ab initio* calculations predict that the fcc $Fe_{50}Cu_{50}$ and $L1_2$ (fcc type) $Fe_{25}Cu_{75}$ phases are relatively stable and likely to be formed. Consequently, the fcc $Fe_{25}Cu_{75}$ and $Fe_{50}Cu_{50}$ solid solution models are set and subjected to annealing at 300 K. The simulation results show that they could retain their original structures. As a typical example, Fig. 4 shows the projections of atomic positions of the FM $Fe_{50}Cu_{50}$ solid solution after annealing at 300 K for 100 000 MD time steps. It can be seen that the initial fcc

TABLE IV. The comparison of physical properties, E_c (eV/atom), a (Å), and bulk modulus B (Mbar), derived from the PM Fe-Cu potential with those from *ab initio* calculation. The fitted parameters, A, B (Å), and C (Å), are also listed.

		Ab initio calculation			Fitted		
Phase	Structure	E_c (eV/atom)	a (Å)	B (Mbar)	E_c (eV/atom)	a (Å)	B (Mbar)
$Fe_{25}Cu_{75}$	$L1_2$	3.47	3.60	1.56	3.46	3.60	1.20
$Fe_{50}Cu_{50}$	B2	3.58	2.82	1.90	3.55	2.82	1.51
A	0.246 957	B		−0.514 729	C		−0.037 315

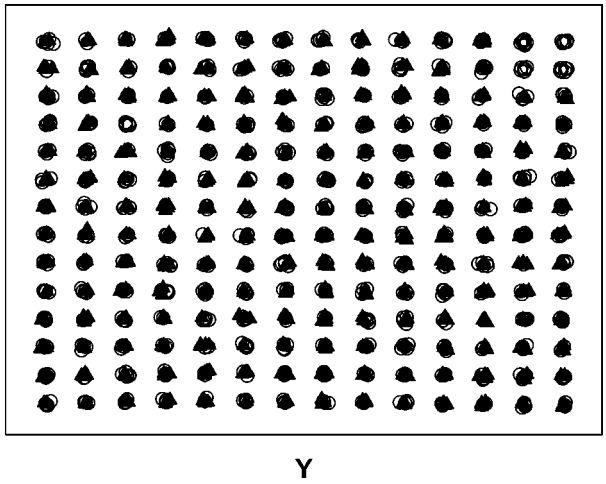

FIG. 4. The projections of atomic positions of the FM $Fe_{50}Cu_{50}$ solid solution after annealing at 300 K for 100 000 MD time steps. Filled triangles: Fe. Open circles: Cu.

structure after random substitution is still retained after annealing at 300 K. Accordingly, some physical properties of the two phases after annealing at 0 K are calculated and listed in Table III together with those from *ab initio* calculations and experiments. Apparently, it can be seen from Table III that the lattice constants of the $Fe_{50}Cu_{50}$ and $Fe_{25}Cu_{75}$ phases determined by three different methods agree well with each other and the cohesive energies of the two Fe-Cu phases are also compatible.

Similar MD simulations with the FM Fe-Cu potential are also conducted for the $Fe_{90}Cu_{10}$ and $Fe_{30}Cu_{70}$ phases with fcc and bcc structures, respectively, and the results are shown in Table V. It can be seen that the bcc $Fe_{90}Cu_{10}$ and the fcc $Fe_{30}Cu_{70}$ phases are more likely to be formed, as they have smaller heats of formation (ΔH_f) than the fcc $Fe_{90}Cu_{10}$ and the bcc $Fe_{30}Cu_{70}$ phases, respectively. Interestingly, a bcc $Fe_{90}Cu_{10}$ and fcc $Fe_{30}Cu_{70}$ alloys were indeed obtained in experiments by mechanical alloying and vapor deposition.[3,7] Moreover, the experimentally determined lattice constants of the bcc $Fe_{90}Cu_{10}$ and the fcc $Fe_{30}Cu_{70}$ alloys were 2.87 and 3.63 Å,[3] respectively, which are also in good agreement with the values of 2.88 and 3.67 Å from the present MD simulation, respectively, providing a supplemental support to the relevance of the newly derived FM Fe-Cu potential.

TABLE V. Physical properties of some metastable Fe-Cu phases derived from the present MD simulation (0 K) with the FM Fe-Cu potential and other works, respectively.

Phase	Method	Structure	a (Å)	ΔH (kJ/mol)
$Fe_{90}Cu_{10}$	MD	fcc	3.66	7.66
	MD	bcc	2.88	6.85
	Expt.	bcc[a,b]	2.87[a]	
$Fe_{30}Cu_{70}$	MD	bcc	2.87	16.25
	MD	fcc	3.67	15.44
	Expt.	fcc[a,b]	3.63[a]	

[a]Reference 3.
[b]Reference 7.

Finally, we discuss whether, or not, the so-called solid-state amorphization (SSA) can take place in the Fe-Cu system. In experiments, only metastable crystalline Fe-Cu alloys of either a fcc or bcc structure have been obtained in a broad composition range, while amorphous Fe-Cu alloy has not been formed by the currently available nonequilibrium producing techniques.[2–4,7–11] Recently, Lin *et al.* proposed a model which predicted that SSA could hardly take place in the Fe-Cu system, as its kinetic factor was lower than a required critical value for SSA.[35] Besides, Ma *et al.* conducted thermodynamic calculation for the Fe-Cu alloys and found out that an amorphous phase had significantly more positive ΔH_f than its fcc and bcc countparts.[11] In the present study, MD simulations with the FM Fe-Cu potential are performed at 300 K for the fcc and bcc Fe-Cu solid solution models over the entire composition range, respectively. It turns out that the fcc and bcc Fe_xCu_{100-x} solid solutions do not collapse and do not transform into amorphous upon annealing for a long time, suggesting that the fcc and bcc solid solutions are energetically favored over their amorphous counterparts. Apparently, the present simulation results are consistent with the reported experimental observations[2–4,7–11] as well as with the thermodynamic predictions.[11,35]

D. Magnetic properties of metastable Fe-Cu phases

In the past decades, there has been long-standing interest in experimental studies concerning the magnetic properties of the metastable Fe-Cu alloys.[2,7,8,10–12,36,37] As to theoretical studies, very recently, *ab initio* calculations have been developed to calculate the magnetic properties of the Fe-Cu alloys under various methods.[14–18] For instance, in 1994, Serena and García conducted linearized augmented-plane-wave calculations to study the ferromagnetism of fcc and bcc Fe-Cu phases under the local-density approximation as well as the local-spin-density approximation.[14] In 1998, Tatarchenko *et al.* used the Korringa–Kohn–Rostoker method within the coherent-potential approximation (CPA) and they found that for the fcc Fe-Cu alloys, an alloying induced low spin to high spin transition took place when the Cu content was above approximately 17 at. %.[15] In 1999, James *et al.* employed the linear muffin tin orbit method within CPA and also observed the low spin to high spin transition.[16] Later, Wang *et al.*, using the self-consistent full-potential linearized augmented-plane-wave (FLAPW) method under the generalized gradient approximation (GGA), discovered that the fcc and bcc Fe-Cu alloys had a ferromagnetic ground state with an enhanced moment at Fe site and expanded volume.[17] Almost concurrent with the work in Ref. 17, Zhang and Ma also conducted FLAPW method within GGA for the fcc and bcc Fe-Cu alloys at six different compositions and observed the enhancement of magnetic moments as well as the magnetovolume expansion upon magnetic interaction between the alloyed Fe and Cu.[18] In the present *ab initio* calculations, we use the projector augmented wave (PAW) method[20] under GGA to calculate the magnetic properties of the Fe_xCu_{100-x} phase ($x=0$, 25, 50, 75, 100). Note that our PAW method is somewhat different from those reported in the literature,[14–18]

TABLE VI. *Ab initio* calculated equilibrium average atomic volume V_0 (Å^3/atom), magnetic moment per Fe atom M_1 (μ_B/Fe atom), and average magnetic moment per metal atom M_2 (μ_B/atom) for some Fe-Cu alloys.

Phase	Structure	V_0 (Å^3/atom)	M_1 (μ_B/Fe atom)	M_2 (μ_B/atom)	Expt. (μ_B/atom)
Fe	bcc	11.333	2.20	2.20	2.22[a]
$Fe_{75}Cu_{25}$	fcc($L1_2$)	11.471	2.18		
	$L6_0$	11.745	2.43		
	A15	11.930	2.49		
	bcc	*11.944*	*2.51*	*1.88*	*1.69*[b]
	$D0_9$	22.479	3.19		
$Fe_{50}Cu_{50}$	*fcc*	*11.958*	*2.65*	*1.33*	*1.09*[b]
	bcc(B2)	12.069	2.54		
	B1	14.085	2.96		
	B3	18.821	3.04		
$Fe_{25}Cu_{75}$	bcc	12.069	2.65		
	fcc($L1_2$)	*12.157*	*2.60*	*0.65*	*0.60*[a]
	$L6_0$	12.216	2.64		
	A15	12.649	3.00		
	$D0_9$	23.549	3.06		
Cu	fcc	12.057			

[a]Reference 11.

[b]Reference 37. For $L6_0$, $c/a=0.863$.

it is of interest see whether or not those observations[17,18] can be reproduced by the present *ab initio* scheme. Moreover, besides the fcc and bcc structures, our calculations are also performed for some Fe-Cu alloys with others simple crystalline structures and some new results are obtained. In the calculations, the lattice constant of the Fe-Cu alloy with each structure is varied to find out the local energy minimum, thus determining the magnetic moment of the Fe-Cu alloy.

The calculated equilibrium average atomic volume and the magnetic moment per Fe atom for each Fe-Cu phase with different structures are listed in Table VI. To compare with the experimental values, the magnetic moment per Fe atom is converted into magnetic moment per metal atom in the alloy and is also listed in Table VI. Several points are worth noting in Table VI. First of all, it can be seen that the calculated Bohr magnetic moments per atom (μ_B/atom) in the fcc $Fe_{25}Cu_{75}$, fcc $Fe_{25}Cu_{50}$, and bcc $Fe_{75}Cu_{25}$ alloys are 0.65, 1.33, and 1.88, respectively, which are in reasonable agreement with the experimentally determined values of about 0.60 for the fcc $Fe_{25}Cu_{75}$,[11] 1.09 for the fcc $Fe_{50}Cu_{50}$,[37] and 1.69 for the bcc $Fe_{75}Cu_{25}$ alloys,[37] respectively. Similar to the results in Refs. 17 and 18, the calculated magnetic moment in the present study is a litter higher than the experimental values. This small positive deviation is perhaps due to the calculation error as well as the error involved in the experiments.[18] Second, the magnetic moment of Fe, as seen in Table VI, is enhanced by the alloying of Cu. Moreover, the magnetovolume effect can be seen in all the Fe-Cu phase with a specific structure, i.e., a larger lattice constant brings about a larger magnetic moment (not shown). These observations are consistent with those in Refs. 17 and 18, confirming the reliability and reproducibility of the predictions from different *ab initio* methods. Third, for a specific Fe-Cu phase ($Fe_{75}Cu_{25}$, $Fe_{50}Cu_{50}$, and $Fe_{25}Cu_{75}$) with different structures, generally speaking, the larger the equilibrium average atomic volume, the larger the magnetic moment per Fe atom. As seen in Table VI, this observation is exactly true for the $Fe_{75}Cu_{25}$ phase, while for the $Fe_{50}Cu_{50}$ and $Fe_{25}Cu_{75}$ phases, the exceptions come from the fcc structures, possibly because the fcc Fe has both low spin and high spin states and its magnetic properties are rather complicated. Finally, among the calculated simple crystalline structures, the highest magnetic moments per Fe atom are 3.19 for $D0_9$ $Fe_{75}Cu_{25}$, 2.96 and 3.04 for B1 and B3 $Fe_{50}Cu_{50}$, as well as 3.00 and 3.06 for A15 and $D0_9$ $Fe_{25}Cu_{75}$, respectively, which are much higher than those of the phases with the experimentally observed structures (bcc $Fe_{75}Cu_{25}$, fcc $Fe_{50}Cu_{50}$, and fcc $Fe_{25}Cu_{75}$), respectively. These calculation results seem to suggest that, in order to get higher magnetic moment, proper experimental techniques should be developed to produce the Fe-Cu phase with a crystalline structure having larger average atomic volume.

IV. CONCLUSION

(1) *Ab initio* calculations are able to predict the structures, lattice constants, and cohesive energies of the metastable $Fe_{25}Cu_{75}$ and $Fe_{50}Cu_{50}$ phases and the predicted properties are in good agreement with the experimental observations reported so far in the literature.

(2) An EAM FM Fe-Cu potential is constructed for the

equilibrium immiscible Fe-Cu system through fitting to some *ab initio* calculated properties. The potential is not only able to reproduce some physical properties of the metastable Fe-Cu phases, but also to properly reflect the structural stability of the system.

(3) Governed by the derived FM Fe-Cu potential, MD simulations show that when $0 \leqslant x \leqslant 60$, the fcc Fe_xCu_{100-x} phase has lower ΔH_f and is more stable than the bcc phase, whereas for the case of $60 < x \leqslant 100$, the bcc Fe_xCu_{100-x} phase becomes energetically favored.

(4) *Ab initio* calculations using the PAW method are also able to determine the magnetic moments of the Fe_xCu_{100-x} phase ($x = 0$, 25, 50, 75, 100), and the calculated results are in reasonable agreement with the experimentally measured values.

ACKNOWLEDGMENTS

The authors are grateful to the financial support from the National Natural Science Foundation of China, The Ministry of Science and Technology of China (through Grant No. 2000067207), as well as from Tsinghua University.

*Author to whom correspondence should be addressed; electronic mail: dmslbx@tsinghua.edu.cn

[1] F. R. deBoer, R. Boom, W. C. M. Mattens, A. R. Miedema, and A. K. Niessen, *Cohesion in Metals: Transition Metal Alloys* (North-Holland, Amsterdam, 1989).
[2] A. R. Yavari, P. J. Desré, and T. Benameur, Phys. Rev. Lett. **68**, 2235 (1992).
[3] J. Eckert, J. C. Holzer, C. E. Krill, and W. L. Johnson, J. Appl. Phys. **73**, 2794 (1993).
[4] K. Uenishi, K. F. Kobayashi, S. Nasu, H. Hatano, K. N. Ishihara, and P. H. Shingu, Z. Metallkd. **83**, 132 (1992).
[5] L. J. Huang and B. X. Liu, Appl. Phys. Lett. **57**, 1401 (1990).
[6] G. W. Yang, W. S. Lai, C. Lin, and B. X. Liu, Appl. Phys. Lett. **74**, 3305 (1999).
[7] C. L. Chien, S. H. Liou, D. Kofalt, W. Yu, T. Egami, and T. R. McGuire, Phys. Rev. B **33**, 3247 (1986).
[8] B. X. Liu and F. Pan, Phys. Rev. B **48**, 10276 (1993).
[9] K. Sumiyama, Y. Yoshitake, and Y. Nakamura, Acta Mater. **33**, 1785 (1985).
[10] E. F. Kneller, J. Appl. Phys. **35**, 2210 (1964).
[11] E. Ma, M. Atzmon, and F. E. Pinkerton, J. Appl. Phys. **74**, 955 (1993).
[12] P. Crespo, A. Hernando, and A. G. Escorial, Phys. Rev. B **49**, 13227 (1994).
[13] E. Ma and M. Atzmon, Mater. Chem. Phys. **39**, 249 (1995).
[14] P. A. Serena and N. García, Phys. Rev. B **50**, 944 (1994).
[15] A. F. Tatarchenko, V. S. Stepanyuk, W. Hergert, P. Rennert, R. Zeller, and P. H. Dederichs, Phys. Rev. B **57**, 5213 (1998).
[16] P. James, O. Eriksson, B. Johansson, and I. A. Abrikosov, Phys. Rev. B **59**, 419 (1999).
[17] J. T. Wang, L. Zhou, Y. Kawazoe, and D. S. Wang, Phys. Rev. B **60**, 3025 (1999).
[18] W. Q. Zhang and E. Ma, J. Mater. Res. **15**, 653 (2000).
[19] G. Kresse and J. Hafner, Phys. Rev. B **47**, 558 (1993).
[20] G. Kresse and D. Joubert, Phys. Rev. B **59**, 1758 (1999).
[21] J. Perdew and A. Zunger, Phys. Rev. B **23**, 5048 (1981).
[22] J. P. Perdew, J. A. Chevary, S. H. Vosko, K. A. Jackson, M. R. Pederson, D. J. Singh, and C. Fiolhais, Phys. Rev. B **46**, 6671 (1992).
[23] H. J. Monkhorst and J. D. Pack, Phys. Rev. B **13**, 5188 (1976).
[24] J. B. Liu, Z. C. Li, and B. X. Liu, Phys. Rev. B **63**, 132204 (2001).
[25] Y. S. Shi, D. Qian, G. S. Gong, X. F. Jin, and D. S. Wang, Phys. Rev. B **65**, 172410 (2002).
[26] M. Parrinello and A. Rahman, J. Appl. Phys. **52**, 7182 (1981).
[27] G. J. Ackland, D. J. Bacon, A. F. Calder, and T. Harry, Philos. Mag. A **75**, 713 (1997).
[28] Y. N. Osetsky and A. Serra, Philos. Mag. A **73**, 249 (1996).
[29] M. S. Daw and I. Baskes, Phys. Rev. Lett. **50**, 1285 (1983).
[30] R. A. Johnson and D. J. Oh, J. Mater. Res. **4**, 1195 (1989).
[31] J. Cai and Y. Y. Ye, Phys. Rev. B **54**, 8398 (1997).
[32] A. M. Guellil and J. B. Adams, J. Mater. Res. **7**, 639 (1992).
[33] H. R. Gong, L. T. Kong, W. S. Lai, and B. X. Liu, Phys. Rev. B **66**, 104204 (2002).
[34] B. J. Lee, M. I. Bakes, H. Kim, and Y. K. Cho, Phys. Rev. B **64**, 184102 (2001).
[35] C. Lin, G. W. Yang, and B. X. Liu, Phys. Rev. B **61**, 15649 (2000).
[36] P. Crespo, A. Hernando, R. Yavari, O. Drbohlav, A. G. Escorial, J. M. Barandiarán, and I. Orúe, Phys. Rev. B **48**, 7134 (1993).
[37] T. Mashimo, X. S. Huang, X. Fan, K. Koyama, and M. Motokawa, Phys. Rev. B **66**, 132407 (2002).